Supporting Information:

JM050276n

A Systematic Analysis of the Effect of Small-Molecule Binding on Protein Flexibility of the Ligand-Binding Sites

Chao-Yie Yang, Renxiao Wang and Shaomeng Wang*

Departments of Internal Medicine and Medicinal Chemistry and Comprehensive Cancer Center, University of Michigan,1500 E. Medical Center Drive, Ann Arbor, MI 48109, USA

Table S1. Average B-factor of all atoms, atoms within 8 Å from the binding site and atoms whose atom depths[1] > 5 Å (Core) based on the backbone (BK) and side chain atoms (S1-4) classification. S1: sp3 Carbon and Sulfur atoms, S2: sp2 Carbon, aromatic carbon, sp2 nitrogen and aromatic nitrogen atoms, S3: charged carbon (Arg), nitrogen (Lys) and oxygen atoms (Glu, Asp), S4: sp3 oxygen (Thr, Ser) and sp2 oxygen atoms. The number in the parentheses is the standard deviation.

	All			< 8 Å			Core		
Type	Free	X	Δ<B>	Free	X	Δ<B>	Free	X	Δ<B>
BK	23.5 (12.3)	19.4 (10.4)	-4.1	23.0 (12.2)	16.5 (8.2)	-6.5	20.5 (9.5)	16.6 (8.0)	-3.9
S1	25.3 (13.8)	21.2 (11.7)	-4.1	24.7 (26.8)	18.0 (9.9)	-6.7	20.4 (9.4)	16.5 (8.0)	-3.9
S2	26.2 (15.3)	22.2 (13.3)	-4.0	26.8 (15.3)	18.8 (10.5)	-8.0	19.2 (9.2)	16.4 (8.0)	-2.8
S3	34.9 (17.7)	30.6 (15.9)	-4.3	31.1 (16.3)	22.2 (12.3)	-8.9	25.4 (15.6)	20.8 (15.9)	-4.6
S4	27.9 (15.2)	23.3 (13.0)	-4.6	27.1 (15.5)	19.1 (9.6)	-8.0	20.9 (9.9)	17.3 (8.7)	-3.6

Table S2. Details information of the crystal structures studied in this work. NF stands for not found. The number in the parentheses in the PDBID (complex) column corresponds to the backbone RMSD between the free and the ligand-bound proteins. The last two columns are the programs used to determine crystal structures.

Protein Names	PDB ID (Free)	Res. (Å)	PH	T (K)	PDB ID (Complex)	Res. (Å)	PH	T(K)	-pKd	ClogP[2]	Volume[3]	MW[2]	Ref.	Prog. Free	Prog. Comp
Chain L, B1-8 Fv Fragment	1a6u	2.0	NF	269	1a6v (0.00) 1a6w(0.66)	1.8 1.8	NF NF	269 269		-4.073 0.827	265.08 223.16	308.29 349.10	4 4	PROLSQ	PROLSQ
Inhibitor And Calcium Bound Domain Vi Of Porcine Calpain	1alv	1.9	7.4	280	1alw(0.37)	2.03	7.4	280	6.52	-0.225	184.71	307.13	5	X-Plor 3.8	X-Plor 3.5
Fk506-Binding Protein	1d6o	1.85	8.0	297	1d7h(0.11) 1d7i(0.15) 1d7j(0.12)	1.90 1.90 1.85	8.0 8.0 8.0	297 297 297	3.30	-1.378 -0.543 -0.839	70.33 105.70 65.21	78.13 124.23 88.11	6 6 6	X-Plor 3.1	X-Plor 3.1
The Cysteine Rich Domain of Mannose Receptor	1dqg	1.7	6.5	120	1dqo(0.33)	2.2	6.5	120		-2.852	227.58	300.26	7	CNS	CNS
E.Coli Cofactor-Dependent Phosphoglycerate Mutase	1e58	1.25	8.5	105	1e59(0.43)	1.3	8.5	105		-1.432	220.41	411.76	8	SHELXL-97	SHELXL-97

Urtica Dioica Agglutinin Isolectin	1ehd	1.5	5.6	286	1ehh(0.61)	1.9	5.6	286		-4.452	509.57	624.57	9	X-Plor 3.1	X-Plor 3.1
da Uncomplexed Form. Crystal Structure Of U	1eis	1.66	6.0	298	1en2(0.61) 1enm(0.32)	1.4 1.9	6.0 6.0	298 298		-4.363 -3.657	668.13 502.22	608.57 810.75	10 10	REFM AC	REFM AC
N-Acetyl Neuramindate Lyase	1f6p	2.25	4.6	113	1f73(0.39) 1f74(1.97) 1f7b(0.27)	1.95 1.6 1.8	4.6 4.6 4.6	113 113 113	2.39 3.05	-5.558 -2.062 -7.654	257.02 249.73 259.92	310.28 292.26 310.28	11 11 11	REFM AC	REFM AC
Fab Fragment Of Monoclonal Antibody (Lnkb-2) Against Human Interleukin-2	1f8t	2.20	5.6	300	1f90(0.95)	2.6	5.6	300		-0.780	928.64	1037.12	12	CNS 0.9	CNS 0.9
The Pleckstrin Homology Domain From Dapp1PHISH	1fao	2.40	7.0	100	1fb8(1.20)	1.8	7.0	100		-7.461	332.82	484.13	13	CNS 0.9	CNS 0.9
O-Succinylbenz oate Synthase from E. Coli	1fhu	1.65	6.75	100	1fhv(1.16)	1.77	NF	100		-5.963	184.21	220.18	14	TNT	CNS
FK506 Binding Protein (FKBP)	1fkk	2.2	NF	NF	1fkj(0.51)	1.7	NF	NF		6.929	736.49	804.02	15	X-Plor	X-Plor
Adipocyte Lipid Binding Protein Mutant	1g7n	1.7	7.0	298	1g74(0.40)	1.5	6.8	113		3.786	284.97	281.45	16	CNS	CNS
Macrophage Migration Inhibitory Factor (Mif)	1gdo	1.50	5.0	100	1gcz(0.12)	1.9	5.0	100	5.13	2.171	196.15	234.20	17	X-Plor 98.1	X-Plor 98.1
Retinol Binding Protein	1hbq	1.7	NF	NF	1hbp(0.27)	1.9	NF	NF		6.657	283.72	288.47	18	X-Plor	X-Plor

Mouse major urinary protein-I	1i04	2.0	NF	100	1i05(0.76) 1i06(0.71)	2.0 1.9	5.8 5.8	298 298		0.432 1.491	145.53 137.08	142.20 143.25	19 19	CNS 0.9	CNS 0.9
Ferric Reductase From Archaeoglobus Fulgidus	1i0r	1.5	8.4	100	1i0s(0.42)	1.65	8.4	100		-21.478	557.296	662.42	20	CNS	CNS
Rnase Hii From Archaeoglobus Fulgidus	1i39	1.95	8.5	93	1i3a(0.38)	2.18	8.5	94		-2.420	113.82	155.07	21	CNS 0.9	CNS 0.9
Thermococcus Litoralis Phosphoglucose Isomerase	1j3q	1.85	4.0	100	1j3r(0.27)	2.18	4.0	100		-5.426	206.13	259.13	22	CNS 1.1	CNS 1.1
Diap1-Bir2	1jd4	2.70	8.0	100	1jd5(0.58) 1jd6(0.54) 1q4q(0.56)	1.9 2.7 2.1	8.5 8.5 5.8	100 100 100	6.62	2.963 3.451 0.042	786.80 810.94 815.84	1021.43 1047.07 1055.10	23 23 24	X-Plor 3.1	X-Plor 3.1[(a)]
Grb2 Sh2 Domain	1jyu	2.75	6.0	290	1jyq(12.64) 1jyr(12.71)	2.0 1.55	6.0 6.0	100 290	8.70	-4.320 -6.559	622.37 900.66	731.14 1197.02	25 25	CNS 1.0	CNS 1.0
Citrobacter Amalonaticus Methylaspartate Ammonia Lyase	1kko	1.33	8.0	100	1kkr(0.41)	2.1	8.0	100		-6.687	124.75	145.11	26	REFMAC	REFMAC
The Mrd Protein	1kmz	1.5	6.0	100	1kll(12.52)	1.5	6.0	100	5.20	-1.045	261.05	320.30	27	SHELXL-97	SHELXL-97
crbp from Zebrafish	1kqx	1.38	5.6	100	1kqw(0.72)	1.7	5.6	100		6.403	287.37	286.45	28	SHELXL-97	SHELXL-97

A snake venom 2 metalloproteinase from Taiwan Habu	1kuf	1.35	4.6	123	1kug(0.32) 1kui(0.29) 1kuk(0.29)	1.37 1.5 1.45	4.6 4.6 4.6	123 123 123	3.80 3.77 3.91	-3.849 -4.477 -5.239	360.94 374.90 385.47	479.44 493.47 493.51	29 29 29	CNS 1.0	CNS 1.0
Leucine Aminopeptidase	1lan	1.9	7.8	123	1lam(0.19)	1.6	7.8	123		-0.888	127.62	119.16	30	X-Plor 3.1	X-Plor 3.1
Adipocyte Lipid-Binding Protein	1lib	1.7	NF	NF	1lic(0.29) 1lid(0.32) 1lie(0.30) 1lif(0.28)	1.6 1.6 1.6 1.6	NF NF NF NF	NF NF NF NF		6.173 3.786 3.212 4.270	289.32 283.77 259.91 287.10	305.50 281.45 255.42 283.47	31 31 31 31	X-Plor + TNT	X-Plor + TNT
Auxin Binding Protein	1lr5	1.9	7.5	100	1lrh(0.19)	1.9	5.5	100	6.82	-1.252	165.17	185.20	32	REFM AC	REFM AC
Human Interleukin-2	1m47	1.99	7.0	100	1m48(0.65)	1.95	7.0	100	5.09	3.249	403.50	447.55	33	REFM AC 5.0	REFM AC 5.1.19
Maltodextrin-Binding Protein	1mpb	2.0	NF	NF	1mpd(3.44)	2.3	NF	NF		-4.399	269.12	342.30	34	X-Plor 3.1	X-Plor 3.1
Calpain Domain 6	1nx2	2.2	NF	103	1nx3(0.20)	2.45	NF	103		-0.225	188.22	307.13	35	CNS	CNS
The Structure Of Bacillus Subtilis Rbsd	1ogc	2.0	6.	295	1ogd(0.09) 1oge(0.10) 1ogf(0.26)	1.95 2.05 2.3	6. 6. 6.	295 295 295		-2.181 -2.613 -1.539	120.32 169.24 82.90	150.13 214.11 92.09	36 36 36	CNS	CNS
Cellular Retinol-Binding Protein Ii	1opa	1.9	NF	NF	1opb(0.64)	1.9	NF	NF		6.403	283.76	286.45	37	X-Plor	X-Plor

T.Gondii Ldh1	1pze	1.95	4.2	100	1pzf(1.39) 1pzg(0.34) 1pzh(1.40)	2.2 1.6 1.9	4.5 4.5 4.5	100 100 100		-5.524 -17.772 -20.118	512.89 512.51 508.52	661.43 661.43 662.42	38 38 38	CNS 1.0	CNS 1.0
The 70 Kda Soluble Lytic Transglycosylase Slt70 From Escherichia Coli	1qsa	1.65	5.0	120	1qte(0.10)	1.9	5.0	120		-3.721	518.47	615.56	39	X-Plor 3.843	X-Plor 3.843
Native Phosphoglucose Isomerase From Pyrococcus Furiosus	1qxj	1.8	5.6	100	1qy4(0.18) 1qxr(0.13)	1.8 1.7	5.6 5.6	100 100		-5.426 -5.257	202.75 179.67	259.13 229.10	40 40	REFMAC 5.0	REFMAC 5.0
Oligo-Peptide Binding Protein (Oppa)	1rkm	2.4	5.5	120	2rkm(3.07) 2olb(3.12)	1.8 1.4	5.5 5.5	120 123	3.90 5.54	-3.622 -4.089	255.40 373.81	290.36 434.53	41 42	REFMAC	REFMAC[(b)]
Human Hsp90 Geldanamycin-Binding Domain	1yer	1.65	NF	113	1yet(0.34)	1.9	NF	113		5.190	498.12	555.68	43	X-Plor	X-Plor
Enolase (E.C.4.2.1.11)	3enl	2.25	NF	NF	4enl(0.19) 5enl(0.19) 6enl(0.19) 7enl(0.89)	1.9 2.2 2.2 2.2	NF NF NF NF	NF NF NF NF		-1.116 -4.962 -4.713 -4.962	 134.34 113.97 131.91	65.39 184.13 154.10 184.13	44 44 44 44	PROLSQ	PROLSQ

(a) 1Q4Q was determined using CNS program.

(b) 2OLB was determined using PROLSQ program.

Figure S1. Histogram distribution of the changes of normalized B-factor after binding for atoms in the proteins within 8 Å from the ligands. B_{norm} = B-factor - <B-factor> / σ , where <B-factor> is the average B-factor of each protein and σ is the standard deviation.

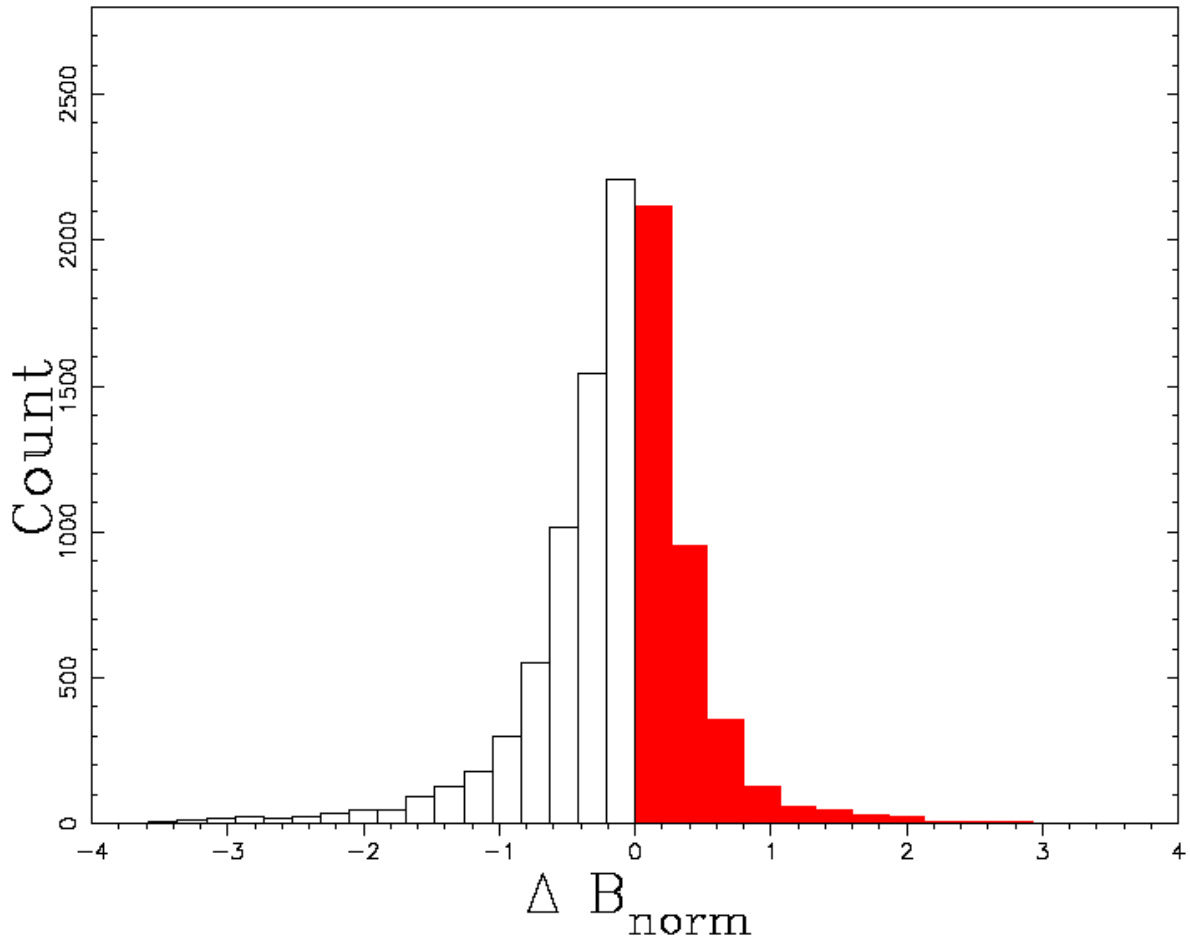

Figure S2. Distribution of ΔB values of the 63 protein-ligand complexes where the x-axis is the ΔB and the y-axis is the counts. PDB ID and temperature of the measurement are displayed at the left and right top corner of the figures. NF: the temperature of the experiment not reported from the literature.

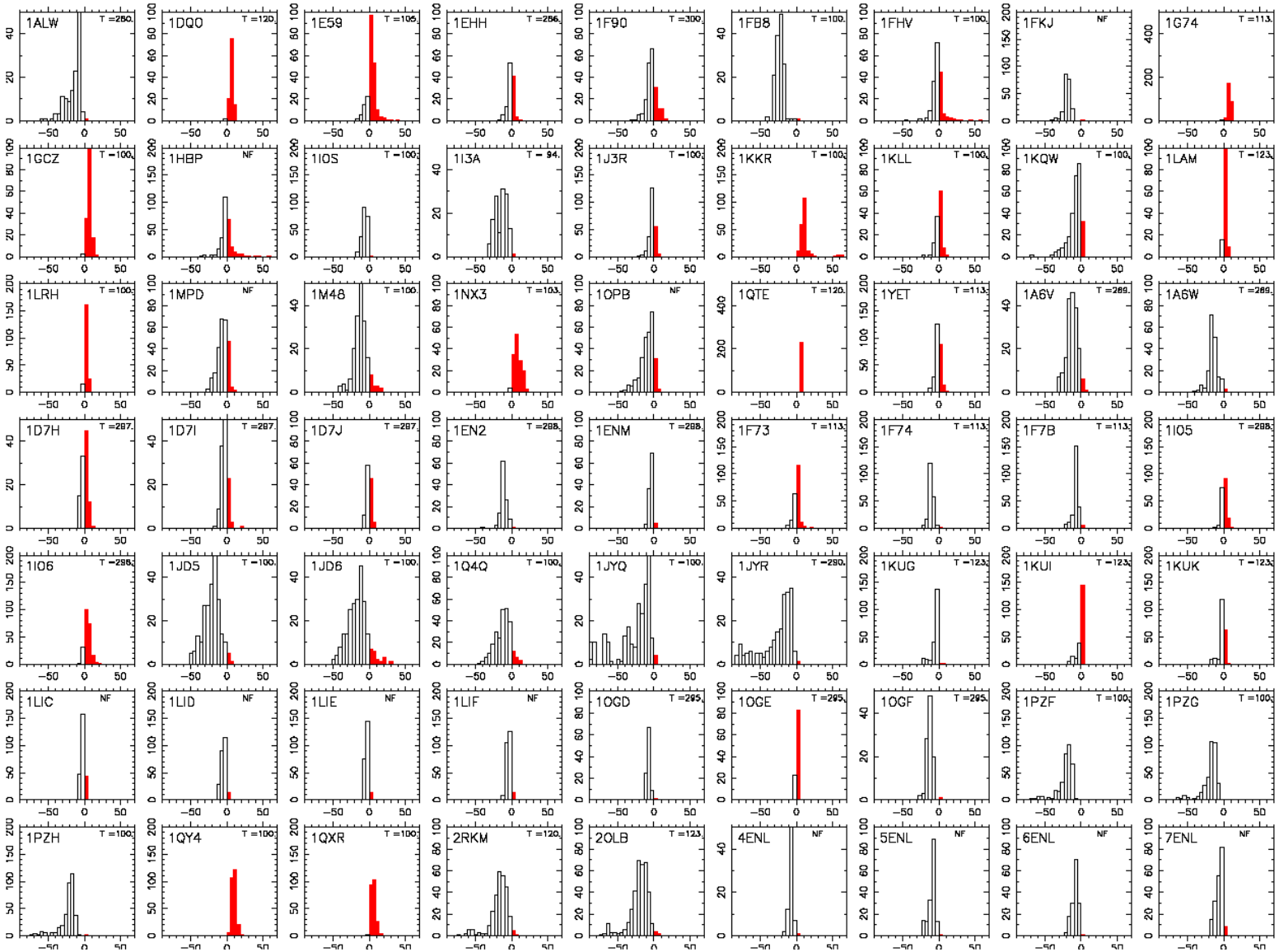

Figure S3. The distribution of the ΔB values for both ligand-free and ligand-bound proteins determined at (a) the same temperature [47 out of 63] and (b) different temperatures or temperature not specified [16 out of 63]. Note that the scale of y-axis was plotted differently.

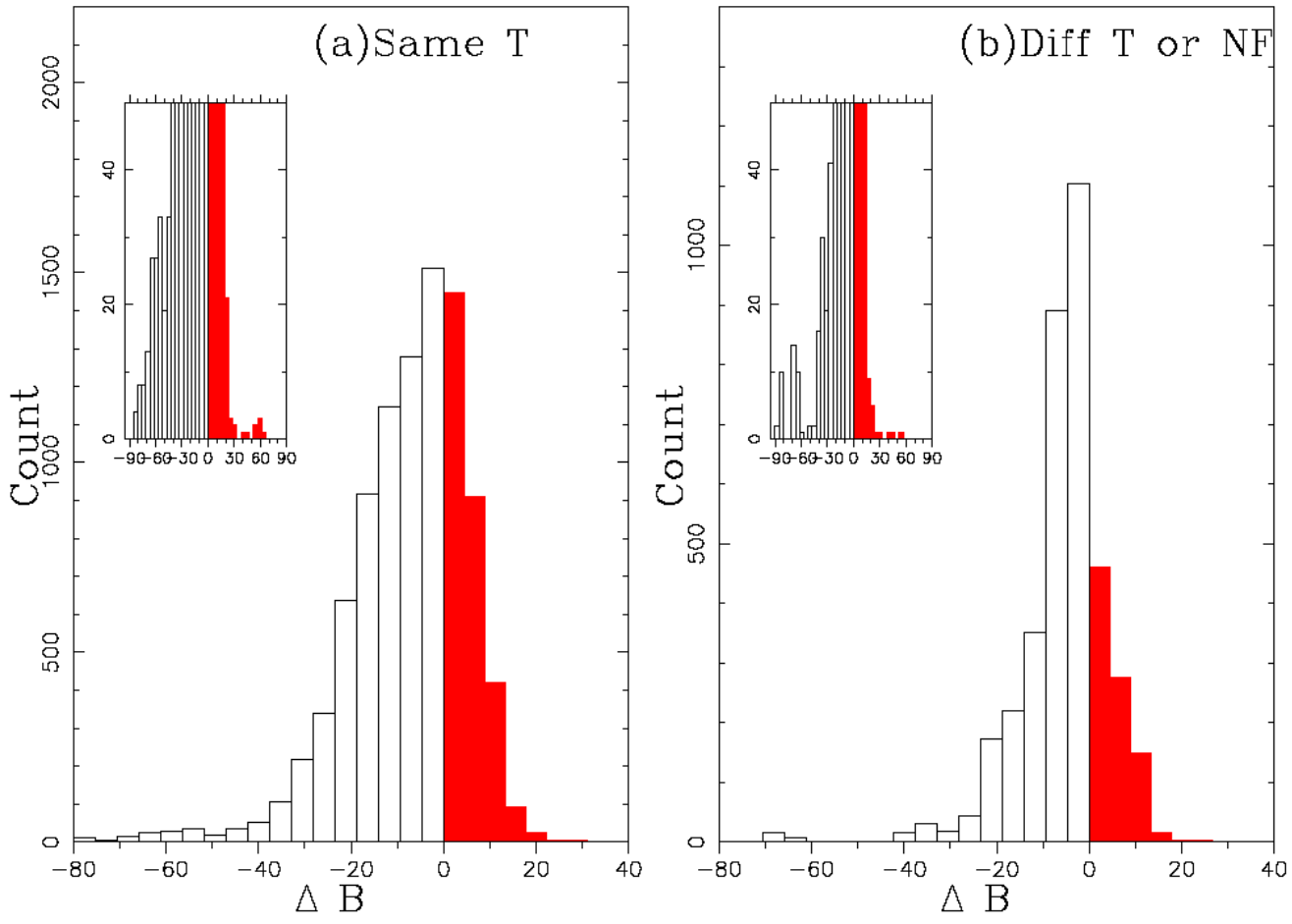

Figure S4. Phylogenic relationship of the 37 proteins studied in this work based on the sequence similarity analysis using BLAST[45].

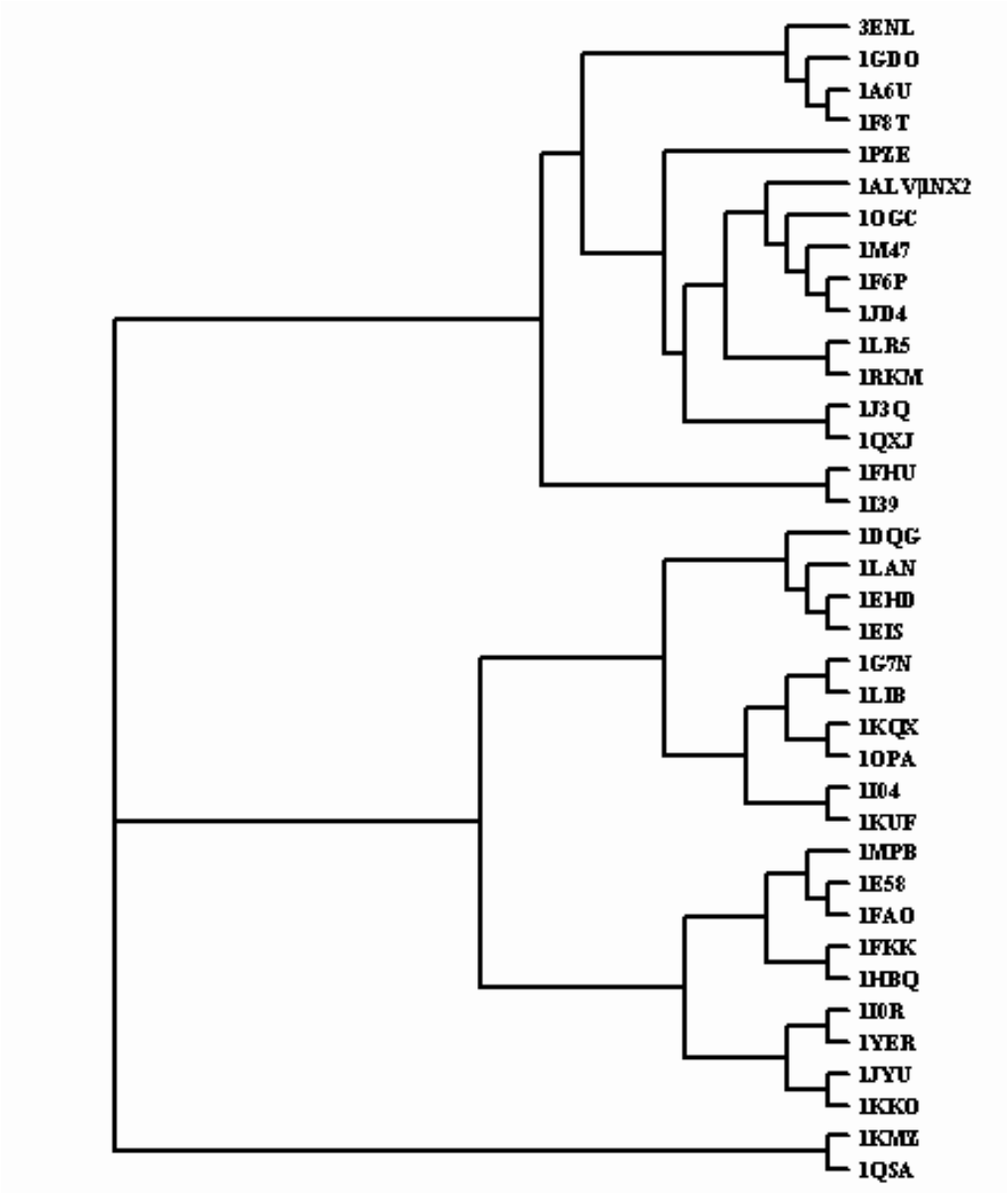

List S1. CATH[46] superfamily classification of the 37 proteins studied in this work.

Immuglobulin: 2 (1A6U,1F8T)

EF-hand: 1 (1ALV)

FKBP-like: 2 (1D6O,1FKK)

Ricin B-like Lectins: 1 (1DQG)

Phosphoglycerate mutase-like: 1 (1E58)

Plant lectins/antimicrobial peptidase: 2(1EHD,1EIS)

Aldolase: 1 (1F6P)

PH-domain like: 1(1FAO)

Enolase C-terminal domain-like: 3 (1FHU,1KKO,3ENL)

Lipocalins: 6(1G7N,1HBQ,1I04,1KQX,1LIB,1OPA)

N-terminal nucleophile aminohydrolase (Ntn hydrolase): 1 (1GDO)

FMN-binding split barrel: 1 (1I0R)

Ribonuclease H-like: 1 (1I39)

Inhibitor of Apoptosis repeat: 1 (1JD4)

SH2 domain: 1 (1JYU)

Glyoxalase/Bleomycin resistance protein/Dihydroxybiphenyl dioxygenase: 1 (1KMZ)

Metalloprotease (“Zincins”), catalytic domain: 1 (1KUF)

Zn-dependent exopeptidase: 1 (1LAN)

RmlC-like cupins: 1 (1LR5)

4-helical cytokins: 1 (1M47)

Periplasmic binding protein like-II: 2 (2RKM,1MPB)

Bacterial muramidase: 1 (1QSA)

ATPase domain of HSP90 chaperone/DNA topoisomerase/Histine kinase: 1 (1YER)

Unkown: 5 (1J3Q,1NX2,1OGC,1PZE,1QXJ)

References:

1. Pintar, A ; Carugo, O. ; Pongor, S. Atom depth in protein structure and function. *Trends Biochem. Sci*., **2003,** *28*, 593-597.

2. Calculated using ChemDraw program. ChemDraw: CambridgeSoft Inc., 100 CambridgePark Drive, Cambridge, MA 02140 USA.

3. Calculated using the Spacefill program in the TINKER package. TINKER: (a) Ren, P.; Ponder, J. W. Polarizable Atomic Multipole Water Model for Molecular Mechanics Simulation. *J. Phys. Chem. B*, **2003**, *107*, 5933. (b) Ren, P.; Ponder, J. W. Consistent treatment of inter- and intramolecular polarization in molecular mechanics calculations. *J. Comput. Chem.*, **2002**, *23*, 1497. (c) Pappu, R. V.; Hart, R. K.; Ponder, J. W. Analysis and Application of Potential Energy Smoothing and Search Methods for Global Optimization. *J. Phys. Chem. B*, **1998**, *102*, 9725. (d) Hodsdon, M. E.; Ponder, J. W.; Cistola, D. P. The NMR solution structure of intestinal fatty acid-binding protein complexed with palmitate: application of a novel distance geometry algorithm. *J. Mol. Biol.*, **1996**, *264*, 585. (e) Kundrot, C. E.; Ponder, J. W.; Richards, F. M. Algorithms for Calculating Excluded Volume and Its Derivatives as a Function of Molecular Conformation and Their Use in Energy Minimization. *J. Comput. Chem.*, **1991**, *12*, 402. (f) Ponder, J. W.; Richards, F. M. An Efficient Newton-like Method for Molecular Mechanics Energy Minimization of Large Molecules. *J. Comput. Chem.*, **1987**, *8*, 1016.

4. Simon, T.; Henrick, K; Hirshberg, M.; Winter, G. Fragment and its (4-hydroxy-3-nitrophenyl) acetate complex of murine B1-8 antibody. *To be published.*

5. Lin, G. D., Chattopadhyay, D; Maki, M; Wang, K. K.; Carson, M.; Jin, L.; Yuen, P. W.; Takano, E.; Hatanaka, M.; DeLucas, L. J.; Narayana, S. V. Crystal structure of calcium bound domain VI of calpain at 1.9 A resolution and its role in enzyme assembly, regulation, and inhibitor binding. *Nat. Struct. Biol*, **1997**, *4*, 539-547.

6. Burkhard, P.; Taylor, P.; Walkinshaw, M.D, X-ray structures of small ligand-FKBP complexes provide an estimate for hydrophobic interaction energies. *J. Mol. Biol.*, **2000**, *295*, 953-962.

7. Liu, Y.; Chirino, A. J.; Misulovin, Z.; Leteux, C; Feizi, T.; Nussenzweug, M. C.; Bjorkman, P. J. Crystal structure of the cysteine-rich domain of mannose receptor complexed with a sulfated carbohydrate ligand. *J. Exp. Med.*, **2000**, *191*, 1105-1116.

8. Bond, C. S.; White, M. F; Hunter, W. N. High resolution structure of the phosphohistidine-activated form of *Escherichia coli* cofactor-dependent phosphoglycerate mutase. *J. Biol. Chem.*, **2001**, *276*, 3247-3253.

9. Harata, K.; Muraki, M. Crystal structures of Urtica dioica agglutinin and its complex with tri-N-acetylchitotriose. *J. Mol. Biol.*, **2000**, *297*, 673-681.

10. Saul, F. A.; Rovira, P.; Boulot, G.; Van Damme, E. J. M.; Peumans, W. J.; Truffa-Bachi, P.;

Bentley, G. A. Crystal structure of Urtica dioica agglutinin, a superantigen presented by MHC molecules of class I and class II. *Structure Fold. Des.*, **2000**, *8*, 593-603.

11. Barbosa, J. A.; Smith, B. J.; Degori, R.; Ooi, H. C.; Marcuccio, S. M.; Campi, E. M.; Jackson, W. R.; Brossmer, R.; Sommer, M.; Lawrence, M.C. Active site modulation in the N-acetylneuraminate lyase sub-family as revealed by the structure of the inhibitor-complexed Haemophilus influenzae enzyme. *J. Mol. Biol.*, **2000**, *303*, 405-421.

12. Fokin, A. V.; Afonin, P. V.; Mikhailova, I. I.; Tsygannik, I. N.; Mareeva, T. I.; Nesmeianov, V. A.; Pangborn, W.; Lee, N.; Duax, W.; Siszak, E.; Pletnev, V. Z. Spatial structure of a Fab-fragment of a monoclonal antibody to human interleukin-2 in two crystalline forms at a resolution of 2.2 and 2.9 angstroms. *Bioorg. Khim.*, **2000**, *26*, 571.

13. Ferguson, K. M.; Kavran, V. G.; Sankaran, V. G.; Fournier, E.; Isakoff, S. J.; Skolnik, E. Y.; Lemmon, M. A. Structural basis for discrimination of 3-phosphoinositides by pleckstrin homology domains. *Mol. Cell*, **2000**, *6*, 373-384.

14. Thompson, T. B.; Garrett, J. B.; Taylor, E. A.; Meganathan, R.; Gerlt, J. A.; Rayment, I. Evolution of enzymatic activity in the enolase superfamily: structure of o-succinylbenzoate synthase from Escherichia coli in complex with Mg2+ and o-succinylbenzoate. *Biochemistry*, **2000**, *39*, 10662-10676.

15. Wilson, K. P.; Yamashita, M. M.; Sintchak, M. D.; Roststein, S. H.; Murcko, M. A.; Boger, J.; Thomson, J. A.; Fitzgibbon, M. J.; Black, J. R.; Navia, M. A. Comparative X-ray structures of the major binding protein for the immunosuppressant FK506 (tacrolimus) in unliganded form and in complex with FK506 and rapamycin. *Acta. Crystallogr. D Biol. Crystallogr*, **1995,** *51*, 511-521.

16. Reese, A. J.; Banaszak, L. J. Specificity determinants for lipids bound to beta-barrel proteins. *J. Lipid Res.*, **2004,** *45*, 232-243.

17. Orita, M.; Yamamoto, S.; Katayama, N.; Aoki, M.; Takayama, K.; Yamagiwa, Y.; Seki, N.; Suzuki, H.; Kurihara, H.; Sakashita, H.; Takeuchi, M.; Fujita, S.; Yamada, T.; Tanaka, A. Coumarin and chromen-4-one analogues as tautomerase inhibitors of macrophage migration inhibitory factor: discovery and X-ray crystallography. *J. Med. Chem.*, **2001**, *44*, 540-547.

18. Zanotti, G.; Berni, R.; Monaco, H. K. Crystal structure of liganded and unliganded forms of bovine plasma retinol-binding protein. *J. Biol. Chem.*, **1993,** *268*, 10728-10738.

19. Timm, D. E.; Baker, L. J.; Mueller, H.; Zidek, L.; Novotny, M. V. Structural basis of pheromone binding to mouse major urinary protein (MUP-I). *Prot. Sci.*, **2001**, *10***,** 997-1004.

20. Chiu, H-J.; Johnson, E., Schroder, I.; Rees, D. C. Crystal structures of a novel ferric reductase from the hyperthermophilic archaeon Archaeoglobus fulgidus and its complex with NADP+. *Structure*, **2001**, *9*, 311-319.

21. Chapados, B. R.; Chai, Q.; Hosfield, D. J.; Qiu, J.; Shen, B.; Tainer, J. A. Structural biochemistry of a type 2 RNase H: RNA primer recognition and removal during DNA replication. *J. Mol. Biol.,* **2001**, *307,* 541-556.

22. Jeong, J.-J.; Fushinobu, S.; Ito, S.; Hidaka, M.; Shoun, H.; Wakagi, T. Characterization of the cupin-type phosphoglucose isomerase from the hyperthermophilic archaeon Thermococcus litoralis. *FEBS Lett.,* **2003**, *535,* 200-204.

23. Wu, J. W.; Cocina, A. E.; Chai, J.; Hay, B. A.; Shi, Y. Structural analysis of a functional DIAP1 fragment bound to grim and hid peptides. *Mol. Cell,* **2001,** *8,* 95-104.

24. Chai, J.; Yan, N.; Huh, J. R.; Wu, J.-W.; Li, W.; Hay, B. A.; Shi, Y. Molecular mechanism of Reaper-Grim-Hid-mediated suppression of DIAP1-dependent Dronc ubiquitination. *Nat. Struct. Biol.,* **2003**, *10,* 892-898.

25. Nioche, P.; Liu, W.-Q., Broutin, I.; Charbonnier, F.; Latreille, M.-T.; Vidal, M.; Boques, B.; Garbay, C.; Ducruix, A. Crystal structures of the SH2 domain of Grb2: highlight on the binding of a new high-affinity inhibitor. *J. Mol. Biol.,* **2002,** *315,* 1167-1177.

26. Levy, C. W.; Buckley, P. A.; Sedelnikova, S.; Kato, Y.; Asano, Y.; Rice, D. W.; Baker, P. J. Insights into enzyme evolution revealed by the structure of methylaspartate ammonia lyase. *Structure,* **2002**, *10,* 105-113.

27. Martin, T. W.; Dauter, Z.; Devedjiev, Y.; Sheffield, P.; Jelen, F.; He, M.; Sherman, D.; Otlewski, J.; Derewenda, Z. S.; Derewenda, U. Molecular basis of mitomycin C resistance in streptomyces: structure and function of the MRD protein. *Structure,* **2002**, *10,* 933-942.

28. Calderone, V.; Folli, C.; Marchesani, A.; Berni, R.; Zanotti, G. Identification and structural analysis of a zebrafish apo and holo cellular retinol-binding protein. *J. Mol. Biol.,* **2002**, *321,* 527-535.

29. Huang, K. F.; Chiou, S. H.; Ko, T. P.; Yuann, J. M.; Wang, A. H. J. The 1.35 A structure of cadmium-substituted TM-3, a snake-venom metalloproteinase from Taiwan habu: elucidation of a TNFalpha-converting enzyme-like active-site structure with a distorted octahedral geometry of cadmium. *Acta. Crystallogr., Sect.D,* **2002**, *58,* 1118-1128.

30. Strater, N.; Lipscomb, W. N. Two-metal ion mechanism of bovine lens leucine aminopeptidase: active site solvent structure and binding mode of L-leucinal, a gem-diolate transition state analogue, by X-ray crystallography. *Biochemistry,* **1995**, *34,* 14792-14800.

31. Xu, Z.; Bernlohr, D. A.; Banaszak, L. J. The adipocyte lipid-binding protein at 1.6-A resolution. Crystal structures of the apoprotein and with bound saturated and unsaturated fatty acids. *J. Biol. Chem.,* **1993**, *268,* 7874-7884.

32. Woo, E. J.; Marshall, J.; Bauley, J.; Chen, J.-G.; Venis, M.; Napier, R. M. Crystal structure of auxin-binding protein 1 in complex with auxin. *Embo J.,* **2002,** *21,* 2877-2885.

33. Arkin, M. A.; Randal, M.; Delano, W. L.; Hyde, J.; Luong, T. N.; Oslob, J. D.; Raphael, D. R.; Taylor, L.; Wang, J.; Wells, J. A.; McDowell, R. S.; Braisted, A. C. Binding of small molecules to an adaptive protein-protein interface. *Proc. Nat. Acad. Sci. USA*, **2003**, *100*, 1603-1608.

34. Hor, L. I.; Shuman, H. A. Genetic analysis of periplasmic binding protein dependent transport in Escherichia coli. Each lobe of maltose-binding protein interacts with a different subunit of the MalFGK2 membrane transport complex. *J. Mol. Biol.*, **1993**, *233*, 659-704.

35. Todd, B.; Moore, D.; Deivanayagam, C. C. S.; Lin, G.-D.; Chattopadhyay, D.; Maki, M.; Wang, K. K. W.; Narayana, S. V. L. A Structural Model for the Inhibition of Calpain by Calpastatin: Crystal Structures of the Native Domain VI of Calpain and its Complexes with Calpastatin Peptide and a Small Molecule Inhibitor. *J. Mol. Biol.*, **2003**, *328*, 131-146.

36. Kim, M.-S.; Shin, J.; Lee, W.; Lee, H.-S.; Oh, B.-H. Crystal Structures of RbsD Leading to the Identification of Cytoplasmic Sugar-binding Proteins with a Novel Folding Architecture. *J. Biol. Chem.*, **2003**, *278*, 28173-28180.

37. Winter, N. S.; Bratt, J. M.; Banaszak, L. J. Crystal structures of holo and apo-cellular retinol-binding protein II. *J. Mol. Biol.*, **1993**, *230*, 1247-1259.

38. Kavanagh, K. L.; Elling, R. A.; Wilson, D. K. Structure of Toxoplasma gondii LDH1: active-site differences from human lactate dehydrogenases and the structural basis for efficient APAD+ use. *Biochemistry*, **2004,** *43*, 879-889.

39. Van Asselt, E. J.; Thunnissen, A.-M. W. H.; Dijkstra, B. W. High resolution crystal structures of the Escherichia coli lytic transglycosylase Slt70 and its complex with a peptidoglycan fragment. *J. Mol. Biol.*, **1999**, *291*, 877-898.

40. Swan, M. K.; Solomons, J. T. G.; Beeson, C. C.; Hansen, T.; Schonheit, P.; Davies, C. Structural evidence for a hydride transfer mechanism of catalysis in phosphoglucose isomerase from Pyrococcus furiosus. *J. Biol. Chem.*, **2003**, *278*, 47261-47268.

41. Sleigh, S. H.; Tame, J. R., Dodson, E. J.; Wilkinson, A. J. Peptide binding in OppA, the crystal structures of the periplasmic oligopeptide binding protein in the unliganded form and in complex with Lysyllysine. *Biochemistry*, **1997**, *36*, 9747-9758.

42. Tame, J. R.; Dodson, E. J.; Murshudov, G.; Higgins, C. F.; Wilkinson, A. J. The crystal structures of the oligopeptide-binding protein OppA complexed with tripeptide and tetrapeptide ligands. *Structure*, **1995**, *3*, 1395-1406.

43. Stebbins, C. E.; Russo, A. A.; Pavletich, N. P. Crystal structure of an Hsp90-geldanamycin complex: targeting of a protein chaperone by an antitumor agent. *Cell*, **1997**, *89*, 239-250.

44. Stec, B.; Lebioda, L. Refined structure of yeast apo-enolase at 2.25 Å resolution. *J. Mol. Biol.*, **1990**, *211*, 235-248.

45. Thompson, J. D.; Higgins, D. G.; Gibson, T. J. CLUSTALW: improving the sensitivity of

progressive multiple sequence alignment through sequence weighting, position-specific gap penalties and weight matrix choice. *Nucleic Acids Res.*, **1994**, *22*, 4673-4680.

46. Orengo, C. A.; Michie, A. D.; Jones, S.; Jones, D. T.; Swindells, M. B.; Thornton, J. M. CATH-a hierarchic classification of protein domain structures. *Structure*, **1997**, *5,* 1093-1108.